World Academy of Science, Engineering and Technology
International Journal of Computer and Information Engineering
Vol:11, No:4, 2017

Sparse-View CT Reconstruction Based on Nonconvex $L_1 - L_2$ Regularizations

Ali Pour Yazdanpanah, Farideh Foroozandeh Shahraki, Emma Regentova

Open Science Index, Computer and Information Engineering Vol:11, No:4, 2017 publications.waset.org/10006930/pdf

***Abstract*—**The reconstruction from sparse-view projections is one of important problems in computed tomography (CT) limited by the availability or feasibility of obtaining of a large number of projections. Traditionally, convex regularizers have been exploited to improve the reconstruction quality in sparse-view CT, and the convex constraint in those problems leads to an easy optimization process. However, convex regularizers often result in a biased approximation and inaccurate reconstruction in CT problems. Here, we present a nonconvex, Lipschitz continuous and non-smooth regularization model. The CT reconstruction is formulated as a nonconvex constrained $L_1 - L_2$ minimization problem and solved through a difference of convex algorithm and alternating direction of multiplier method which generates a better result than L_0 or L_1 regularizers in the CT reconstruction. We compare our method with previously reported high performance methods which use convex regularizers such as TV, wavelet, curvelet, and curvelet+TV (CTV) on the test phantom images. The results show that there are benefits in using the nonconvex regularizer in the sparse-view CT reconstruction.

***Keywords*—**Computed tomography, sparse-view reconstruction, $L_1 - L_2$ minimization, non-convex, difference of convex functions.

I. Introduction

COMPUTED Tomography (CT) is used as a screening method for medical diagnostics, non-destructive testing and airport security. For medical, security or industrial applications of CT a limited number of views is an option for whether reducing the radiation dose or screening time, and obviously the operation cost. In applications, such as non-destructive testing or inspection of a large object, like a turbine or a cargo container one angular view can take up to a few minutes for only one slice. Furthermore, some views could be simply unavailable due to the system configuration. On the other hand, exposure to radiation is a concern in medical CT, specifically when the frequency of test is high [1].

A computed tomography system can be modelled as a linear system in two different scenarios: Noise-free (1) and noisy (2):

$$A\mathrm{x} = b. \tag{1}$$

$$A\mathrm{x} + n = b. \tag{2}$$

where $b \in R^N$ is the projection data, $\mathrm{x} \in R^M$ is the reconstruction image, $A \in R^{N \times M}$ is the system geometry matrix, and n is the approximation of the interference of noise, error, and other factors present in a practical imaging process.

Ali Pour Yazdanpanah is with the Department of Electrical and Computer Engineering, University of Nevada, Las Vegas, NV, 89154 USA (e-mail: pouryazd@unlv.nevada.edu).

TABLE I
PSNR (dB) Values for All the Methods in Our Experiment

Method	SheppLogan	FORBILD
Wavelet	19.2	22.0
Curvelet	26.6	28.7
TV	31.4	29.6
CTV	37.7	36.2
Proposed	39.8	38.7

The reconstruction problem can be solved using a constrained optimization problem,

$$\underset{\mathrm{x}}{\text{minimize}} \ \|\mathrm{x}\|_0 \quad \text{subject to} \quad A\mathrm{x} = b \tag{3}$$

Here l_0-norm is denoted by $\|.\|_0$. Minimizing the L_0 norm is equivalent to finding the sparsest solution and since L_0 minimization is NP-hard [2], a popular approach is to replace L_0 by a convex L_1 norm, which often gives a satisfactory sparse solution.

Assuming noise and given the sparse-view model, the reconstruction problem is ill-posed for minimizing the least-squares function. Therefore, the following cost function with a regularization term has been considered.

$$\underset{\mathrm{x}}{\text{minimize}} \ \|\phi(\mathrm{x})\|_1 \quad \text{subject to} \quad \|b - A\mathrm{x}\|_2^2 \leq \sigma \tag{4}$$

where ϕ is a sparsifying transform and σ is an upper bound of the uncertainty in the projections (b). Here l_1-norm is denoted by $\|.\|_1$ and l_2-norm by $\|.\|_2$. The constrained optimization in (3) is equivalent to the following unconstrained optimization problem [3], [4]:

$$\underset{\mathrm{x}}{\text{minimize}} \ \frac{1}{2}\|b - A\mathrm{x}\|_2^2 + \lambda\|\phi(\mathrm{x})\|_1 \tag{5}$$

where $\lambda > 0$ is a balancing constant which relies on the sparsity of the underlying image x under linear transformation. In (5), the L_1 norm represents the convex relaxation of L_0 that counts the nonzeros. Such matrix A has incoherent column vectors. Considering the problem, the convex sparsifying term $\phi(\mathrm{x})$ can include different regularizers. In the past few years, research efforts have been made to exploring efficient and stable convex regularizers.

The total variation as a convex regularizer have been widely used in the area of image denoising and restoration [5], [6], sparse-view CT reconstruction, and interior tomography [7]-[9]. Transform based methods are proposed generally for inverse problems and CT reconstruction [10]-[13]. Wu et al. [11] introduced to use curvelet as the convex sparsifying transform in the CT reconstruction framework. Curvelet



Fig. 1 Left: SheppLogan phantom, Right: FORBILD head phantom

transform, proposed by Candes [10] in 2002 has better L_1-norm sparsity than that by wavelets and does not generate the staircase-type noise which make it very suitable for sparse-view CT reconstruction. In 2016, a new regularization model for CT reconstruction has been proposed by combining regularization methods based on TV and the curvelet transform (CTV) [14]. It was demonstrated that the method has had superior quality of CT reconstruction when compared to the above mentioned methods.

Recently, there has been a flow of attempts [15]-[17] in developing nonconvex regulaizers to promote sparsity while solving the linear system. Although nonconvex regularizers are generally more challenging to minimize, they have advantages over convex L_1 norm, since convex L_1 norm regularizers do not perform well on practical problems with coherent A matrix. Nonconvex functions were introduced as substitutes to L_0. The quasi-norm (L_q : $q < 1$) [18], [19] and the log-det functional [20] are two examples of these nonconvex functions.

Esser et al. in [21] have first addressed the $L_1 - L_2$ minimization in the context of nonnegative least square problems with applications to spectroscopic imaging. In [15], [17], authors studied the use of a nonconvex functional $L_1 - L_2$ for compressed sensing application and proved the convergence of the nonconvex optimization.

In this paper, we study a nonconvex, Lipschitz continuous and non-smooth regularization model by considering the difference of L_1 and L_2 norms for CT reconstruction. We compare it with a number of CT reconstruction methods including methods using convex regulaizers such as TV, wavelet, curvelet, and CTV.

The paper is organized as follows: In Section II, the nonconvex model for computed tomography system is formulated and the optimization problem is presented. Results are demonstrated in Section III. Conclusions are drawn in Section IV.

II. Method

A constrained $L_1 - L_2$ minimization problem can be defined by replacing L_0 in (3) with $L_1 - L_2$:

$$\underset{\mathrm{x}}{\text{minimize}} \ \|\mathrm{x}\|_1 - \|\mathrm{x}\|_2 \quad \text{subject to} \quad A\mathrm{x} = b \tag{6}$$

In the optimization problem, to minimize $L_1 - L_2$, a difference of convex algorithm (DCA) [22] is utilized. DCA includes linearization of the nonconvex term (second term) in the cost function to raise a new term by solving the L_1-norm subproblem

$$\mathrm{x}^{k+1} = \underset{\mathrm{x}}{\text{argmin}} \ \left\{ \|\mathrm{x}\|_1 - \left\langle p^k, \mathrm{x} \right\rangle \quad \text{s.t.} \quad A\mathrm{x} = b \right\} \tag{7}$$

where $p^k = \frac{\mathrm{x}^k}{\|\mathrm{x}^k\|_2}$.

The DCA method handles the minimization of a cost function in a form of $Q(\mathrm{x}) = f(\mathrm{x}) - g(\mathrm{x})$. $f(\mathrm{x})$ and $g(\mathrm{x})$ are lower semi-continuous convex functions, $f - g$ is a DC decomposition of Q. g and f are considered as DC components of Q. In the DCA method, we build two sequences x^k and z^k as nominees for primal and dual optimal solutions. They are computed by iterating over the following equations:

$$\begin{cases} \mathrm{z}^k \in \partial g(\mathrm{x}^k) \\ \mathrm{x}^{k+1} = \underset{\mathrm{x}}{\text{argmin}} \ f(\mathrm{x}) - (g(\mathrm{x}^k) + \left\langle z^k, \mathrm{x} - \mathrm{x}^k \right\rangle) \end{cases} \tag{8}$$

where z^k is a subgradient of $g(x)$ at x^k.

The unconstrained minimization for (6):

$$\underset{\mathrm{x}}{\text{minimize}} \ \frac{1}{2}\|b - A\mathrm{x}\|_2^2 + \lambda(\|\mathrm{x}\|_1 - \|\mathrm{x}\|_2) \tag{9}$$

The unconstrained cost function in (9) has the following DC decomposition:

$$Q(\mathrm{x}) = \left(\frac{1}{2}\|b - A\mathrm{x}\|_2^2 + \lambda\|\mathrm{x}\|_1 \right) - \lambda\|\mathrm{x}\|_2 \tag{10}$$

Considering $|\mathrm{x}\|_2$ is differentiable with gradient $\frac{\mathrm{x}}{\|\mathrm{x}\|_2}$ and for $\mathrm{x} = 0$, $0 \in \partial|\mathrm{x}\|_2$, the following can be written:

$$\mathrm{x}^{k+1} = \begin{cases} \underset{\mathrm{x}}{\text{argmin}} \ \frac{1}{2}\|b - A\mathrm{x}\|_2^2 + \lambda\|\mathrm{x}\|_1 & if \ \ \mathrm{x}^k = 0 \\ \underset{\mathrm{x}}{\text{argmin}} \ \frac{1}{2}\|b - A\mathrm{x}\|_2^2 + \lambda\|\mathrm{x}\|_1 - \left\langle x, \lambda \frac{\mathrm{x}^k}{\|\mathrm{x}^k\|_2} \right\rangle & otherwise \end{cases} \tag{11}$$

In each DCA iteration, the following L_1-norm convex subproblem is solved:

$$\underset{\mathrm{x}}{\text{minimize}} \ \frac{1}{2}\|b - A\mathrm{x}\|_2^2 + \lambda\|\mathrm{x}\|_1 - \left\langle \mathrm{x}, u \right\rangle \tag{12}$$

Equation (12) can be solved using alternating direction of multiplier method (ADMM) [23]. First (12) can be rewritten as

$$\underset{\mathrm{x}}{\text{minimize}} \ \frac{1}{2}\|b - A\mathrm{x}\|_2^2 + \lambda\|v\|_1 - \left\langle \mathrm{x}, u \right\rangle \quad s.t. \quad \mathrm{x} - v = 0 \tag{13}$$

Then we create the Lagrangian as

$$\begin{aligned} \mathcal{L}(\mathrm{x}, v, \rho) = \frac{1}{2}\|b - A\mathrm{x}\|_2^2 + \lambda\|v\|_1 - \left\langle \mathrm{x}, u \right\rangle \\ + \rho^T(\mathrm{x} - v) + \frac{\eta}{2}\|\mathrm{x} - v\|_2^2 \end{aligned} \tag{14}$$

where η is the penalty parameter and ρ is the Lagrangian multiplier. ADMM iterations are as:

Open Science Index, Computer and Information Engineering Vol:11, No:4, 2017 publications.waset.org/10006930/pdf

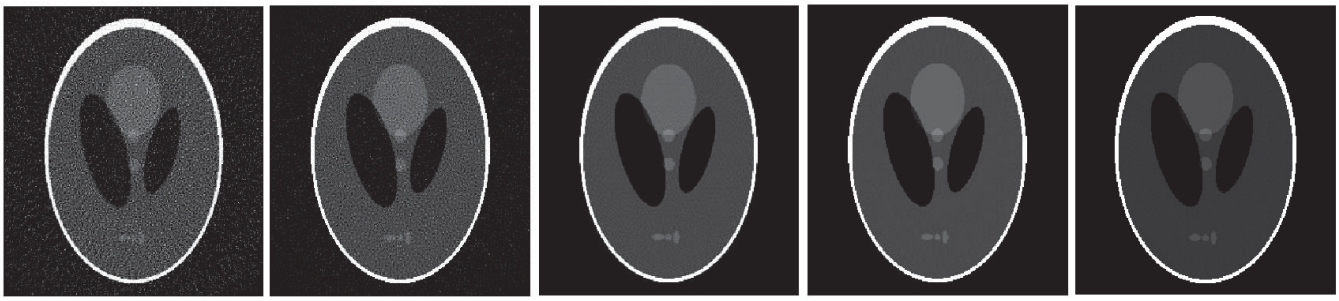


Fig. 2 Left to right: SheppLogan phantom reconstruction result using Wavelet, Curvelet, TV, CTV, and the proposed methods

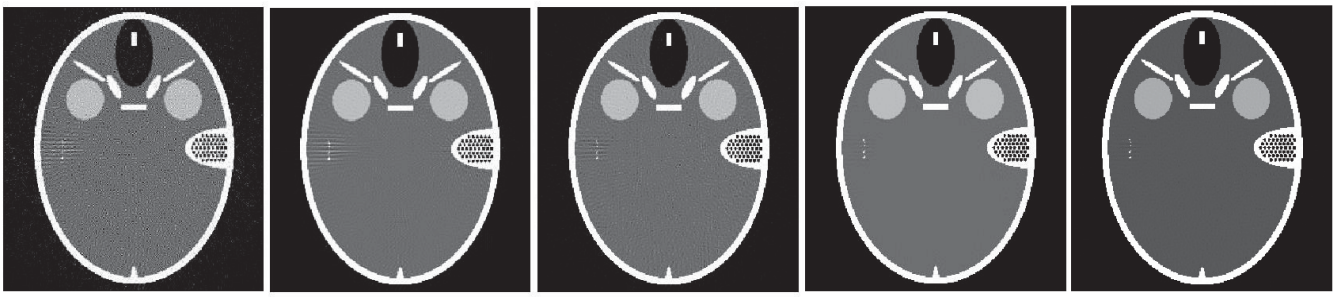


Fig. 3 Left to right: FORBILD head phantom reconstruction result using Wavelet, Curvelet, TV, CTV, and the proposed methods

Open Science Index, Computer and Information Engineering Vol:11, No:4, 2017 publications.waset.org/10006930/pdf

$$\begin{cases} \mathrm{x}^{i+1} = \underset{\mathrm{x}}{\operatorname{argmin}}\ \mathcal{L}(\mathrm{x}, v^i, \rho^i) \\ v^{i+1} = \underset{\mathrm{v}}{\operatorname{argmin}}\ \mathcal{L}(\mathrm{x}^{i+1}, v, \rho^i) \\ \rho^{i+1} = \rho^i + \eta(\mathrm{x}^{i+1} - v^{i+1}) \end{cases} \tag{15}$$

The closed-form solution for v in the second step of (15) can be found using a shrinkage operator:

$$v^{i+1} = shrink(\frac{\mathrm{x}^{i+1} + \rho^i}{\eta}, \frac{\lambda}{\eta}) \tag{16}$$

where

$$shrink(x, \xi)_n = sign(x_n).max\left\{|x_n| - \xi, 0\right\} \tag{17}$$

Since A matrix is not a square matrix and thus the normal inversion cannot be obtained, the conjugate gradient method [24] has been chosen as a solution for the first step of (15).

A pseudo-code of the solution for each DCA iteration in (12) is depicted here.

Define $\mathrm{x}^0, v^0, \rho^0$
for $i = 1, 2, ..., iteration$
$\mathrm{x}^{i+1} = \underset{\mathrm{x}}{\operatorname{argmin}}\ \mathcal{L}(\mathrm{x}, v^i, \rho^i)$
$v^{i+1} = shrink(\frac{\mathrm{x}^{i+1} + \rho^i}{\eta}, \frac{\lambda}{\eta})$
$\rho^{i+1} = \rho^i + \eta(\mathrm{x}^{i+1} - v^{i+1})$
end.

Algorithm 1: DCA iteration solution

III. Results

We evaluate the method on two sets simulated data, i.e., SheppLogan phantom [25] and the head phantom which is built based on the work by FORBILD group [26] (Fig. 1). The data have the size of 256×256 pixels and they are simulated with only 100 equally spaced projections. We have reconstructed these phantoms using five methods: Four previously reported high performance methods with convex regulaizers including TV-based regularization (TV), wavelet-based regularization (Wavelet), curvelet-based regularization (Curvelet), curvelet+TV regularization (CTV), and the presented method. Figs. 2 and 3 show the outcomes of the methods, i.e., a substantial reduction of visible artifacts by the proposed method. The peak signal-to-noise ratio (PSNR) represents the objective metrics presented in Table I, and also demonstrates the high performance achieved by the developed method.

IV. Conclusion

The paper has presented a nonconvex, Lipschitz continuous and non-smooth regularization model for CT reconstruction by considering the difference of L_1 and L_2 norms. In our method, a nonconvex constrained $L_1 - L_2$ CT reconstruction problem is formulated. We have used an approach of combining difference of convex algorithm, and alternating direction method of multiplier (ADMM) to solve the formulated optimization problem. The performance of the method has been demonstrated based on the presented images for visual evaluation. The visible artifacts are greatly reduced and the improvement in objective quality over the reference methods is visible. Objectively, PSNR values are also higher that proves a higher performance of the developed method.

Acknowledgment

This work was supported by NASA EPSCoR under cooperative agreement No. NNX10AR89A.

Open Science Index, Computer and Information Engineering Vol:11, No:4, 2017 publications.waset.org/10006930/pdf

REFERENCES

[1] Brenner DJ J., Hall EJ.: Computed tomography: an increasing source of radiation exposure. N Engl J Med. 357(22), 2277–2284 (2007).
[2] Natarajan, B.K.: Sparse approximate solutions to linear systems. SIAM J. Com- put., 227234 (1995).
[3] Goldstein T., Osher S.:The split Bregman method for L1 regular- ized problems. SIAM J. Imag. Sci. 2(2), 323–343 (2009).
[4] Vandeghinste B., Goossens B., Holen R. V., Vanhove C., Pizurica A., Vandenberghe S., Staelens S.: Iterative CT Reconstruction Using Shearlet-Based Regularization. IEEE Trans Nuclear Science. 60(5), 3305–3317 (2013).
[5] Oliveira J.P., Bioucas-Dias J. M., Figueiredo M.A.T.: Adaptative total variation image deblurring: A majorization-minimization approach. Signal Process., 89, 1683–1693 (2009).
[6] Beck A., Teboulle M.: Fast gradient-based algorithms for constrained total variation image denoising and deblurring problems. IEEE Trans. Image Process. 18(11), 2419–2434 (2009).
[7] Sidky E. Y., Pan X.: Image reconstruction in circular cone-beam computed tomography by constrained, total-variation minimization. Phys. Med. Biol. 53(17), 4777–4807 (2008).
[8] Herman G. T., Davidi R.: On image reconstruction from a small number of projections. Inv. Probl. 24(4), 45011–45028 (2008).
[9] Yang J., Yu H., Jiang M., Wang G.: High-order total variation minimization for interior tomography. Inv. Probl. 26(3), 035013 (2010).
[10] Starck JL, Candes EJ, Donoho DL.:The curvelet transform for image denoising. IEEE Trans Image Process. 11(6), 670–84 (2002).
[11] Wu, H., Maier, A., Hornegger, J.: Iterative CT reconstruction using curvelet-based regularization. In: Meinzer, H.-P., Deserno, T.M., Handels, H., Tolxdorff, T. (eds.) Bildverarbeitung fur die Medizin. Springer, Heidelberg (2013).
[12] Pour Yazdanpanah A., Regentova E. E., Bebis G.: Algebraic iterative reconstruction-reprojection (AIRR) method for high performance sparse-view CT reconstruction. Applied mathematics & information sciences. 10(6), 2007–2014 (2016).
[13] Pour Yazdanpanah A., Regentova E. E.: Compressed sensing MRI using curvelet sparsity and nonlocal total variation: CS-NLTV. IS&T 29th International Symposium on Electronic Imaging (2017).
[14] Pour Yazdanpanah A., Regentova E. E.: Sparse-View CT Reconstruction using Curvelet and TV-based Regularization. 13th International Conference Image Analysis and Recognition (ICIAR), Vol. 9730, 672–677 (2016).
[15] Yin, P., Lou, Y., He, Q., Xin, J.: Minimization of L1 L2 for compressed sensing. SIAM J. Sci. Comput., 37(1), A536–A563 (2014).
[16] Lou, Y., Yin, P., He, Q., Xin, J.: Computing sparse representation in a highly coherent dictionary based on difference of L1 and L2. J. Sci. Comput. 64(1), 178–196 (2014).
[17] Yifei, L., Osher, S., and Xin, J.: Computational cspects of constrained L1-L2 minimization for compressive sensing. Modelling, Computation and Optimization in Information Systems and Management Sciences, 169–180 (2015).
[18] R. Chartrand: Exact reconstruction of sparse signals via nonconvex minimization, IEEE Signal Process. Lett., 14, 707–710 (2007).
[19] R. Chartrand and V. Staneva Restricted isometry properties and nonconvex compressive sensing, Inverse Problems, 24, 1–14 (2008).
[20] E. Candes, M. Wakin, and S. Boyd: Enhancing sparsity by reweighted L1 minimization, J. Fourier Anal. Appl., 14, 877–905 (2008).
[21] E. Esser, Y. Lou, and J. Xin, A method for finding structured sparse solutions to non-negative least squares problems with applications, SIAM J. Imaging Sci., 6, 2010–2046 (2013).
[22] Pham-Dinh T., Le-Thi H.A.: Convex analysis approach to d.c. programming: Theory, algorithms and applications. Acta Math. Vietnam. 22(1), 289–355 (1997).
[23] S. Boyd, N. Parikh, E. Chu, B. Peleato, and J. Eckstein, Distributed optimization and statistical learning via the alternating direction method of multipliers, Foundations and Trends in Machine Learning, 3(1), 1–122 (2011).
[24] Hestenes M. R., Stiefel E.: Methods of conjugate gradients for solving linear systems. J. Res. Nat. Bureau Stand. 49(6), 409–436 (1952).
[25] Shepp L.A., Logan B. F.: Reconstructing interior head tissue from X-ray transmissions. IEEE Trans. Nucl. Sci. 21(1), 228–236 (1974).
[26] FORBILD group, http://www.imp.uni-erlangen.de/phantoms/head/head.html, Accessed on 01/10/2016.